Partially Unfolded Equilibrium State of Hen Lysozyme Studied by Circular Dichroism Spectroscopy

Kenji Sasahara, Makoto Demura, and Katsutoshi Nitta*

Division of Biological Sciences, Graduate School of Science, Hokkaido University, Sapporo, Hokkaido 060-0810, Japan

Received November 5, 1999; Revised Manuscript Received March 21, 2000

ABSTRACT: Equilibrium unfolding of hen egg white lysozyme as a function of GdnCl concentration at pH 0.9 was studied over a temperature range 268.2−303.2 K by means of CD spectroscopy. As monitored by far- and near-UV CD at 222 and 289 nm, the lack of coincidence between two unfolding transition curves was observed, which suggests the existence of a third conformational species in addition to native and unfolded states. The three-state model, in which a stable intermediate is populated, was employed to estimate the thermodynamic parameters for the GdnCl-induced unfolding. It was found that the transition from the native to intermediate states proceeds with significant changes in enthalpy and entropy due to an extremely cooperative process, while the transition from the intermediate to unfolded states shows a low cooperativity with small enthalpy and entropy changes. These results indicate that the highest energy barrier for the GdnCl-induced unfolding of hen lysozyme is located in the process from the native state to the intermediate state, and this process is largely responsible for the cooperativity of protein unfolding.

The thermodynamic aspects of partially unfolded intermediate species are important in the understanding of the mechanisms of protein folding/unfolding process (*1*−*3*). Much effort has focused upon the structural and dynamic characterization of the intermediates of protein folding or unfolding, and then molten globules states have been observed under equilibrium conditions and as a kinetic intermediate of refolding in some proteins (*4*−*8*). Although there is much experimental evidence for intermediates, there has been considerable debate about the role of such species. In particular, whether they assist in directing folding efficiently or whether they result from the existence of kinetic traps in the folding reaction has recently emerged as a major question (*9*−*13*). Thus, the elucidation of the role of intermediate states has been a major focus in the study of protein folding/unfolding process.

Kinetic and equilibrium aspects for folding or unfolding of hen egg white lysozyme have been under extensive investigations (*14*, *15*). The GdnCl-induced[1] equilibrium unfolding of hen lysozyme has been regarded as a highly cooperative two-state reaction, which has led to an assumption of the absence of any intermediate states between the native and the unfolded states (*16*, *17*). This behavior of hen lysozyme has been contrasted to that of homologous α-lactalbumin, which forms stable equilibrium intermediates under mildly denaturing conditions (*18*). The intermediate state of α-lactalbumin, commonly called a molten globule state, is characterized by the presence of nativelike secondary structure, a compact shape, the formation of a hydrophobic core exposed to solvent, and the absence of rigid side-chain packing (*18*). The equilibrium molten globule state of α-lactalbumin has been shown to be similar to or identical with a kinetic intermediate transiently accumulated at an early stage of refolding from the unfolded state (*19*, *20*). It has been shown that hen lysozyme also folds via a similar structural intermediate by a stopped-flow CD and by NMR studies on hydrogen-exchange protection (*19*−*22*).

Recently, some stable intermediates have been reported for lysozymes from other species, such as equine and human, and structures of these intermediate states show molten globule features (*23*−*25*). Furthermore, the experimental evidences for intermediates of hen lysozyme have been recently documented in the literature. For example, Haezebrouck et al. (*24*) have suggested the existence of partially unfolded state, which has some characteristics of the molten globule state of homologous α-lactoalbumin, in the thermal unfolding process of lysozyme at lower pH. The small-angle X-ray scattering study reported by Chen et al. (*26*) has suggested the existence of an equilibrium intermediate in the urea-induced unfolding of hen lysozyme at pH 2.9. These results prompted us to look for the partially unfolded states of hen lysozyme in GdnCl-induced equilibrium unfolding. In this study, we investigated the GdnCl-induced unfolding of hen lysozyme to characterize its intermediate over a temperature range 268.2−303.2 K by CD spectroscopy.

MATERIALS AND METHODS

Hen egg white lysozyme (crystallized six times) was purchased from Seikagaku Corporation, Ltd., Tokyo, Japan, and used without further purification. Biochemical-grade GdnCl was purchased from Wako Pure Chemical Industries., Ltd., Osaka, Japan. GdnCl stock solution and buffer stock solution (0.2M HCl) were prepared. The concentration of GdnCl was determined by the diffrence between the refractive index of GdnCl solution and that of water (*27*). Lysozyme was dissolved into both stock solutions. Both stock solutions were adjusted to pH 0.9 by adding HCl with HORIBA pH meter M-8s. The concentration of lysozyme

* To whom correspondence should be addressed. Phone: +81-11-706-2773. Fax: +81-11-706-4992. E-mail: nitta@sci.hokudai.ac.jp.

[1] Abbreviation: GdnCl, guanidinium chloride; CD, circular dichroism; N, native; I, intermediate; U, unfolded.

10.1021/bi992560k CCC: $19.00
Published on Web 05/03/2000

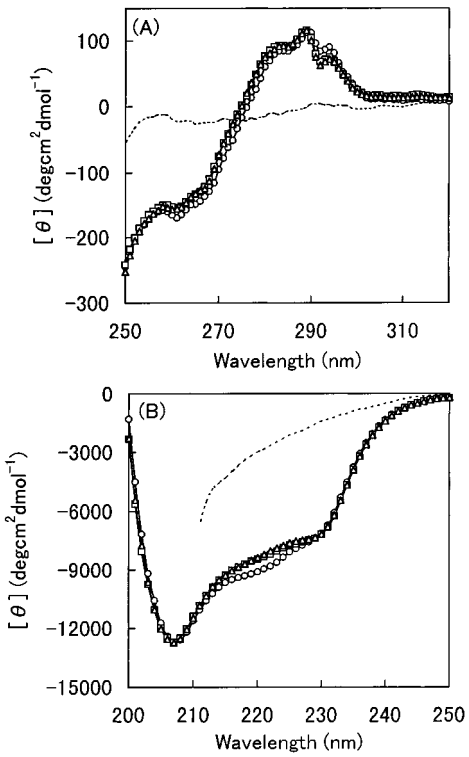

FIGURE 1: Effect of HCl on the conformation of hen lysozyme at 298.2 K, as monitored by near-UV CD (A) and by far-UV CD (B). Circles, pH 2.85; squares, pH 0.9; triangles, pH 0.64; dashed line, pH 0.9 in 6 M GdnCl.

in both solutions was about 28 μM and determined by using an extinction coefficient (37 600 mol^{-1} cm^{-1}) at 280 nm. The distilled and deionized water was used for preparing solutions. For GdnCl-induced unfolding experiment, 30 sample solutions with different GdnCl concentrations were prepared volumetrically from buffer and GdnCl stock solutions. These sample solutions were incubated at room temperature for 15 h.

The GdnCl-induced unfolding of lysozyme was detected by CD measurement with a Jasco J-725 spectropolarimeter. Ellipticities at 289 nm and at 222 nm were measured in quartz cells with 10 and 1 mm path lengths, respectively. The temperature surrounding the cell was maintained within 0.1 K by circulating an ethylene glycol−water mixture from a constant-temperature bath. After measurements have been made, the pH values of the solutions in the transition region were measured to ensure that a constant pH had been maintained.

RESULTS

Figure 1 shows the dependence of mean molar ellipticities of hen lysozyme on wavelength in the low pH region at 298.2 K. The addition of acid (HCl) to the protein solution has little significant effect on aromatic CD at 289 nm, while the intensity of ellipticity monitored at 222 nm is decreased by 8.8% from pH 2.8 to 0.64. Thus, hen lysozyme retains its nativelike near- and far-UV CD spectra up to pH as low as 0.64 and requires high concentration of denaturant for unfolding. It is known that T4 lysozyme, chicken lysozyme, chymotrypsinogen, ubiquitin, and concanavalin A are resistant to high concentrations of acid, and they maintain nativelike far- and near-UV CD spectra over the range pH 7−1 or in some cases lower pH (*28*). We examined the GdnCl-induced equilibrium unfolding of hen lysozyme by CD measurements under the experimental condition pH 0.9, where native lysozyme molecules are destabilized due to electrostatic repulsion, etc. (*29*).

The ellipticities at 289 and 222 nm were measured in the presence of 30 different concentrations of GdnCl. The former reflects the tertiary structure, and the latter reflects mainly the helical content. Sixteen isothermal equilibrium unfolding curves of hen lysozyme were collected over a temperature range 268.2−303.2 K to estimate the thermodynamic parameters for the GdnCl-induced unfolding. The transition curves above 303.2 K and below 268.2 K were not collected because the baseline of the native protein (pretransition region) became too short for accurate analysis due to the thermal denaturation and the solution freezing, respectively.

Figure 2 shows the equilibrium unfolding curves of hen lysozyme at several temperatures. Data are plotted as an apparent fraction of unfolded protein, f_{app}, versus the concentration of GdnCl. The f_{app} values were calculated according to eq 1:

$$f_{app} = (\theta_N - \theta)/(\theta_N - \theta_U) \quad (1)$$

where θ_N, θ_U, and θ are the ellipticities of the protein for the native state (pretransition), for the unfolded state (posttransition region), and in the transition region. The θ_N and θ_U in the transition region were obtained by extrapolation of the linear dependence of the ellipticity on the denaturant concentration in the regions before and after the transition, respectively. The lack of coincidence of the two transition curves by the CD ellipticities at 222 and 289 nm was observed over the temperature range studied, which suggests the existence of the intermediate state during the GdnCl-induced unfolding. We assumed a three-state transition where three state, the native (N), the intermediate (I), and the unfolded (U) states are required for interpreting the transition curves.

The observed ellipticity of the protein [$A_{obs}(c)$] at any denaturant concentration is given by the sum of the contributions from the three states as

$$A_{obs}(c) = A_N f_N(c) + A_I f_I(c) + A_U f_U(c) \quad (2)$$

where $f_N(c)$, $f_I(c)$, and $f_U(c)$ are the fractions of the three states at a GdnCl concentration of c ($f_N + f_I + f_U = 1$), and A_N, A_I, and A_U are the ellipticity values of the N, I, and U states, respectively. The 16 isothermal GdnCl-induced unfolding data over the temperature range 268.2−303.2 K were fitted by the method of nonlinear least-squares to a three-state transition model as follows. The equilibrium constants, K_{NI}, K_{NU}, and K_{IU}, of the GdnCl-induced unfolding transitions from N to I, from N to U, and from I to U are related to the corresponding free-energy differences, ΔG_{NI}, ΔG_{NU}, and ΔG_{IU}:

$$K_{NI} = \exp(-\Delta G_{NI}/RT)$$

$$K_{NU} = \exp(-\Delta G_{NU}/RT)$$

$$K_{IU} = \exp(-\Delta G_{IU}/RT) \quad (3)$$

where R and T are the gas constant and the absolute temperature, respectively. The free-energy differences of the

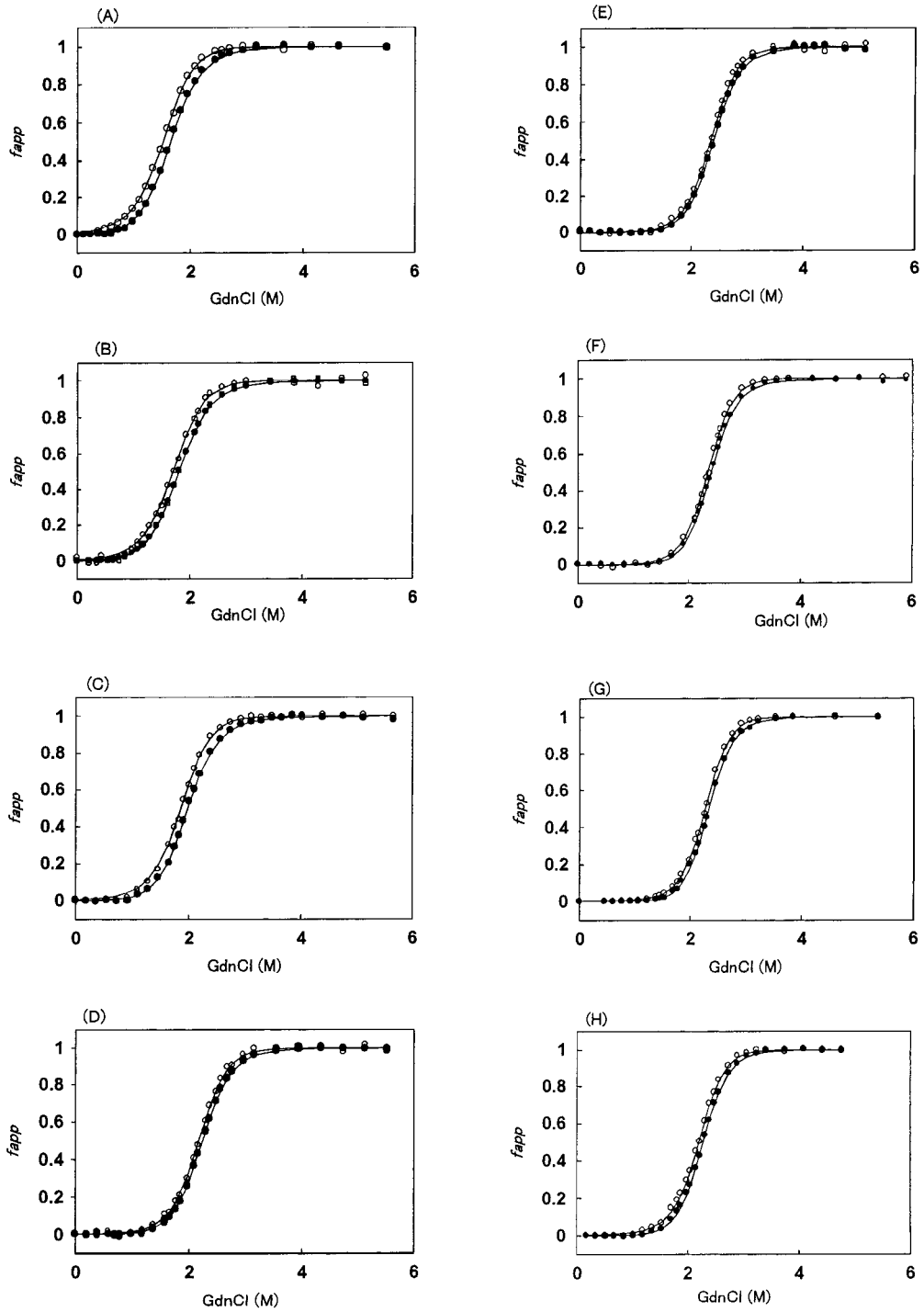

FIGURE 2: Apparent unfolded fraction, f_{app}, of hen lysozyme at pH 0.9 estimated from the ellipticities at 289 nm (open circles) and at 222 nm (filled circles) as a function of GdnCl concentration. (A) 303.2 K, (B) 300.7 K, (C) 298.2 K, (D) 290.7 K, (E) 283.2 K, (F) 278.2 K, (G) 273.2 K, (H) 268.2 K.

respective transitions, ΔG_{NI}, ΔG_{NU}, and ΔG_{IU}, are known to vary approximately linearly with GdnCl concentration c (*30*):

$$\Delta G_{NI} = \Delta G^0_{NI} - m_{NI}c$$

$$\Delta G_{NU} = \Delta G^0_{NU} - m_{NU}c$$

$$\Delta G_{IU} = \Delta G^0_{IU} - m_{IU}c \qquad (4)$$

where m_{NI}, m_{NU}, and m_{IU} represent the cooperativity indexes of the respective transitions, and ΔG^0_{NI}, ΔG^0_{NU}, and ΔG^0_{IU} are ΔG_{NI}, ΔG_{NU}, and ΔG_{IU} at 0 M GdnCl, respectively. The fractions of the N, I, and U states are given by

$$f_N = 1/(1 + K_{NI} + K_{NU})$$

$$f_I = K_{NI}/(1 + K_{NI} + K_{NU})$$

$$f_U = K_{NU}/(1 + K_{NI} + K_{NU}) \qquad (5)$$

Figure 3 shows the theoretical curves of the three fractions, f_N, f_I, and f_U, derived from the three-state transition model based on eqs 2−5.

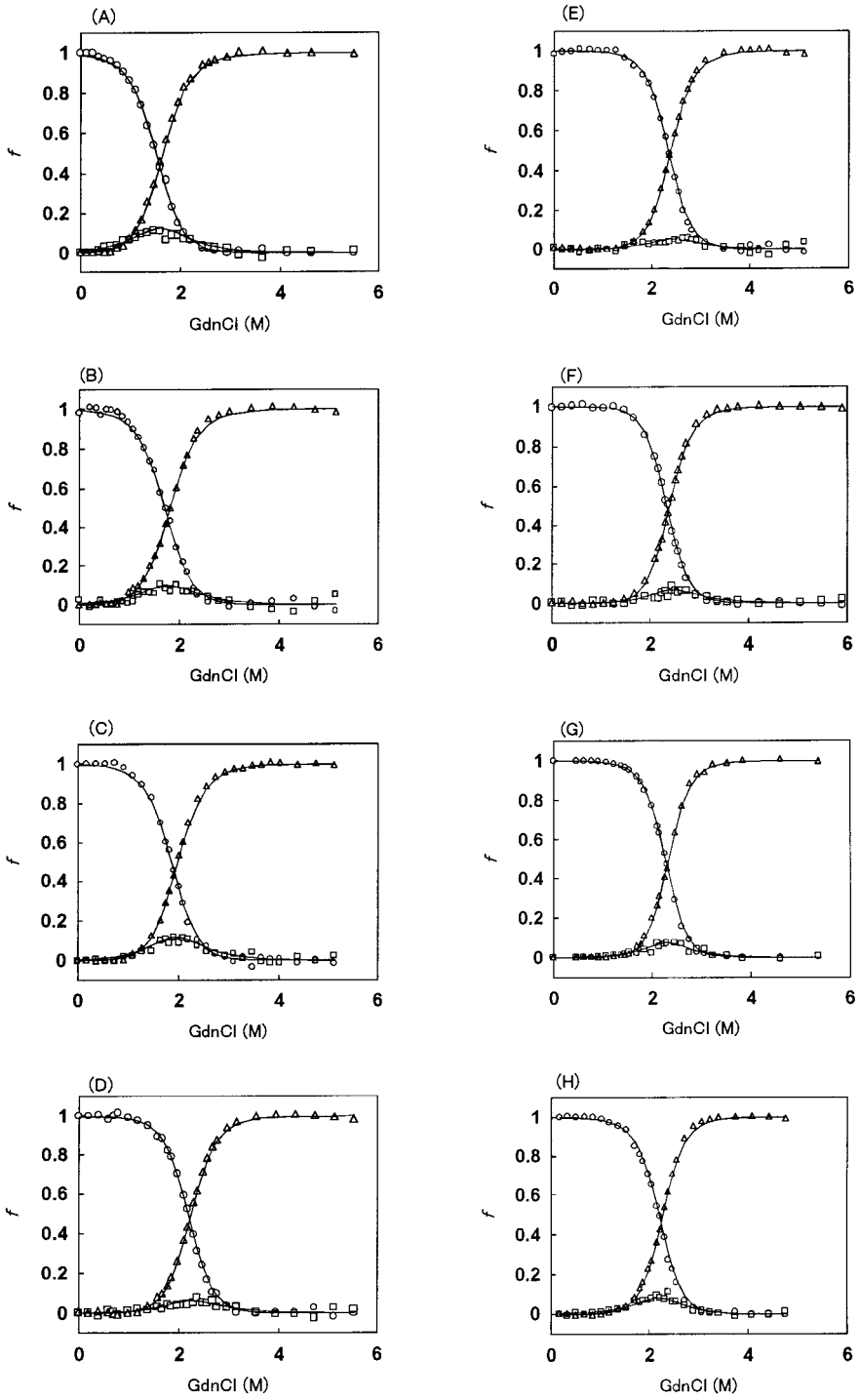

FIGURE 3: Population of the N, I, and U states as a function of GdnCl concentration. (A) 303.2 K, (B) 300.7 K, (C) 298.2 K, (D) 290.7 K, (E) 283.2 K, (F) 278.2 K, (G) 273.2 K, (H) 268.2 K. Circles, f_N; squares, f_I; triangles, f_U. Continuous lines represent the theoretical curves derived from the three-state transition model on the basis of equations 3−5. Marks represent the population derived from the experimental data in Figure 2, assuming $f_N = 1 - f_{app,289}$, $f_I = f_{app,289} - f_{app,222}$, and $f_U = f_{app,222}$, where $f_{app,289}$ and $f_{app,222}$ are the apparent fractions of unfolded protein monitored by near- and far-UV CD at 289 and 222 nm, respectively.

For the evaluation of fitting errors, an apparent effect due to baselines tracing (θ_N and θ_U, respectively) should be included in eq 1 used to fit the spectroscopic data (*31*). We have performed the three-state and the two-state analyses of the unfolding profiles to see whether there are significant deviations from the two-state behavior or not. Figure 4 provides the difference between the two-state versus three-state fit for the representative data at 298.2 K. A small but significant difference is seen in the two analyses, which indicates that the GdnCl-induced unfolding of hen lysozyme at pH 0.9 is well represented by the three-state mechanism in which only N, I, and U states are populated. The mean molar ellipticities of the intermediate state, A_I, in the transition region at 298.2 K are shown in Figure 5, which were calculated by eq 2 from the observed ellipticities, the fractions derived from the three-state transition model, and the native and unfolded baselines of the transition curves. The intermediate state monitored by two CD ellipticities of

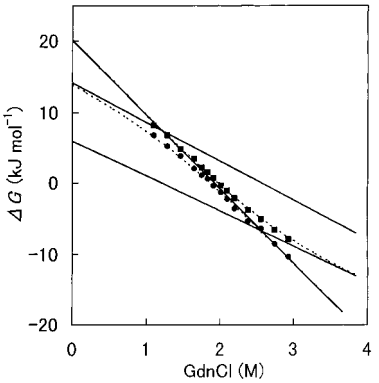

FIGURE 4: Difference between the two-state versus three-state analyses for the GdnCl-induced unfolding data at 298.2 K. Filled circles, ΔG_{NU} from N to U of the two-state transition monitored by CD ellipticity at 289 nm; filled squares, ΔG_{NU} from N to U of the two-state transition monitored by CD ellipticity at 222 nm. The dotted lines through ΔG_{NU} data represent the nonlinear least-squares fit to the experimental data. The linear solid lines represent ΔG_{NU}, ΔG_{NI}, and ΔG_{IU} derived from the three-state transition model, which yielded values for ΔG^0_{NU}, ΔG^0_{NI}, ΔG^0_{IU}, m_{NU}, m_{NI}, and m_{IU} of 20.1 kJ mol^{-1}, 14.1 kJ mol^{-1}, 6.0 kJ mol^{-1}, 10.4 kJ mol^{-1} M^{-1}, 5.5 kJ mol^{-1} M^{-1}, and 4.9 kJ mol^{-1} M^{-1}, respectively.

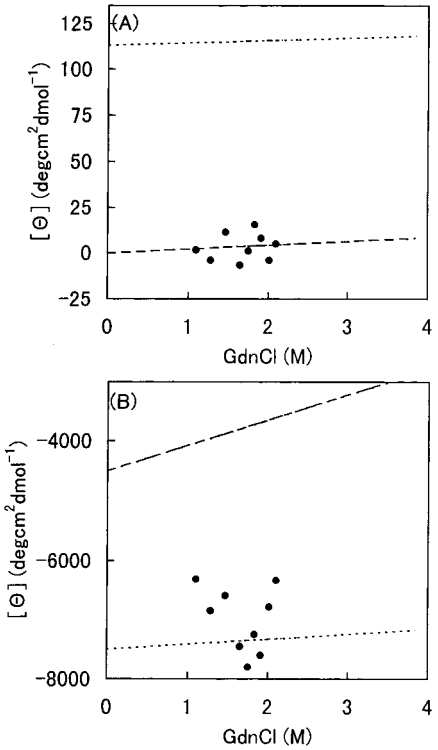

FIGURE 5: Mean molar ellipticities (filled circles) of the intermediate state in the transition region, A_I, monitored by 289 nm (A) and by 222 nm (B) at 298.2 K. The A_I values were calculated by eq 2 from the observed ellipticities, the fractions derived from the three-state model, and the native and unfolded baselines of the transition curves. The dotted and long dashed lines represent the native and unfolded baselines, A_N and A_U, respectively, which were obtained by extrapolation of the linear dependence of the ellipticity on the denaturant concentration in the region before and after the transition.

hen lysozyme is characterized by the presence of nativelike secondary structure and the absence of detectable tertiary structure. These results support that the lack of coincidence between two transition curves cannot be explained in terms of a baseline effect alone, and the two transition curves provide reliable evidence for the presence of a populated

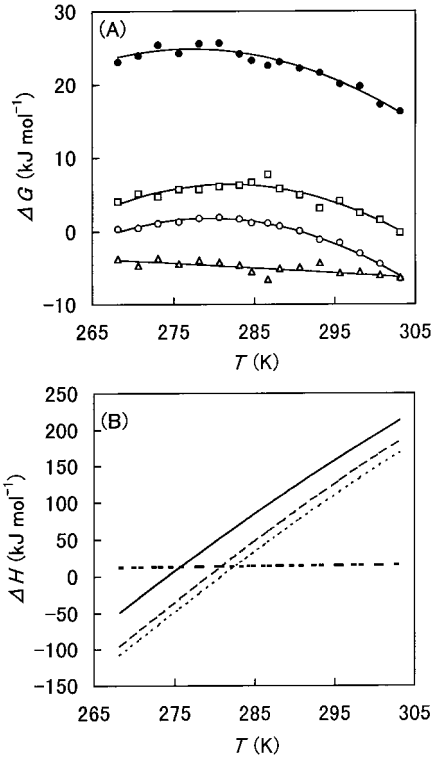

FIGURE 6: (A) Temperature dependence of free-energy changes derived from three-state transition model. Open circles, ΔG_{NU} at 2.2M GdnCl; open squares, ΔG_{NI} at 2.2M GdnCl; open triangles, ΔG_{IU} at 2.2M GdnCl; filled circles, ΔG^0_{NU} at 0 M GdnCl. The continuous lines through the ΔG data represent the fitting curves based on eq 6, where $A = -967 \pm 41$, $B = -270\,000 \pm 12\,000$ K, $C = 0.53 \pm 0.04$ for ΔG_{NU}, $A = -954 \pm 114$, $B = -268\,000 \pm 32\,000$ K, $C = 2.6 \pm 0.1$ for ΔG_{NI}, $A = -13 \pm 110$, $B = -2000 \pm 31\,000$ K, $C = -2.1 \pm 0.1$ for ΔG_{IU}, $A = -902 \pm 108$, $B = -247\,000 \pm 31\,000$ K, $C = 10.1 \pm 0.1$ for ΔG^0_{NU}. (B) Temperature dependence of enthalpy change for the GdnCl-induced unfolding of hen lysozyme. Continuous line, ΔH^0_{NU} at 0 M GdnCl; long dashed line, ΔH_{NU} at 2.2 M GdnCl; dashed line, ΔH_{NI} at 2.2 M GdnCl; thick dashed line, ΔH_{IU} at 2.2 M GdnCl. Enthalpy changes were calculated from the fitting curves of ΔG in Figure 6A according to the eq 7.

equilibrium intermediate in the GdnCl-induced unfolding of hen lysozyme at pH 0.9.

The thermodynamic parameters (ΔG_{NI}, ΔG_{NU}, ΔG_{IU}) of hen lysozyme for the N, I, and U states at GdnCl concentration of 2.2 M, where the I state can be accumulated at a level sufficient for characterization, were calculated in the temperature range 268.2−303.2 K. The temperature dependence of these parameters is shown in Figure 6 A. The plots of ΔG_{NI} and ΔG_{NU} versus temperature show a perceptible curvature, while the stabilization energy, ΔG_{IU}, of the I state appears to increase without a salient curvature as temperature decreases.

If the heat capacity change, ΔC_P, is assumed to be independent of temperature, the Gibbs' free energy change, ΔG, can be expressed in terms of three unknown parameters (A, B, and C), and these parameters can be estimated from experimental data by using the least-squares method (*32*):

$$\Delta G/RT = A \ln(T/T_0) + B(1/T - 1/T_0) + C \qquad (6)$$

where $T_0 = 285.65$ K. The continuous curves in Figures 6A were drawn according to eq 6 with the least-squares best fit

Table 1: Thermodynamic Parameters for GdnCl-Induced Unfolding of Hen Lysozyme at pH 0.9 and 298.2 K[a]

	transition process		
	N→I	I→U	N→U
ΔH^0_{NU} (kJ mol^{-1})			181 (±10)
ΔS^0_{NU} (J K^{-1} mol^{-1})			547 (±40)
$\Delta C^0_{p,NU}$ (kJ K^{-1} mol^{-1})			7.5 (±0.9)
ΔH (kJ mol^{-1})	135 (±17)	16 (±14)	151 (±3)
ΔS (J K^{-1} mol^{-1})	448 (±58)	73 (±50)	520 (±6)
ΔC_p (kJ K^{-1} mol^{-10}	7.9 (±1.0)	0.1 (±0.8)	8.0 (±0.4)

[a] ΔH^0_{NU}, ΔS^0_{NU}, and $\Delta C^0_{p,NU}$ are values at 0 M GdnCl. ΔH, ΔS, and ΔC_P are values at 2.2 M GdnCl. Numbers in parentheses denote standard deviations.

values of *A*, *B*, and *C*. These curves of ΔG for the entire temperature range (268.2−303.2 K) were then applied to eqs 7−9 to determine the enthalpy change, ΔH, the entropy change, ΔS, and the heat capacity change, ΔC_P:

$$\Delta H = \partial(\Delta G/T)/\partial(1/T) \quad (7)$$

$$\Delta S = (\Delta H - \Delta G)/T \quad (8)$$

$$\Delta C_p = (\partial \Delta H/\partial T) \quad (9)$$

Figure 6B shows the temperature dependence of the ΔH values between the N, I, and U states. The transition from the N to the I states for the GdnCl-induced unfolding is accompanied by extensive heat absorption, i.e., it is an extremely cooperative process. On the other hand, the transition between the I and U states shows a low cooperativity with small enthalpy change. The thermodynamic quantities of each transition evaluated at 298.2 K are summarized in Table 1. The transition from the N to the U states in the absence of GdnCl provides ΔH^0_{NU} value of 181 (±10) kJ mol^{-1} and ΔS^0_{NU} value of 547 (±40) J K^{-1} mol^{-1} at 298.2 K, which are almost consistent with the literature values (*33*, *34*) obtained with differential scanning calorimetry, taking into account the experimental uncertainty and the different experimental conditions.

DISCUSSION

Our results from CD measurements provide evidence for a thermodynamically stable intermediate in the GdnCl-induced equilibrium unfolding of hen lysozyme at pH 0.9. This intermediate is indicated from the lack of coincidence between the GdnCl-induced curves measured by far- and near-UV CD at 222 and 289 nm. It has been shown experimentally that in many cases urea- or GdnCl-induced transitions of hen lysozyme can be described in terms of a two-state transition model, which has led to an assumption of the absence of any intermediate states between the native and the unfolded states (*16*, *17*). Analysis of differential scanning calorimetry for the heat-induced unfolding of this protein has indicated that no significant deviations from the equilibrium two-state unfolding mechanism occur (*33*, *35*, *36*). It follows then that hen lysozyme represents a single cooperative macroscopic system in the denaturant-induced and heat-induced equilibrium unfolding where the constituent structural domains do not change their states independently. These results have been attributed to the tight packing at the interface between the α and β domains, which, as a result, behave as a single cooperative unit in hen lysozyme (*36*).

However, evidence for intermediates in equilibrium unfolding of this protein has been documented in the literature. For instance, thermal unfolding curves are not identical as observed by CD measurements at 222 and 270 nm at pH 1.0, which suggested a population of ∼25% of the intermediate (*24*). The small-angle X-ray scattering study reported by Chen et al. (*26*) has suggested the existence of an equilibrium intermediate in the urea-induced unfolding of hen lysozyme at pH 2.9. Hence, one can say that hen lysozyme, which has been considered as a protein of cooperative two-state unfolding behavior, latently reveals a noncooperative unfolding behavior under an extreme condition such as lower pH.

As discussed by Tanford (*14*) and by Robson and Pain (*37*), whether the equilibrium intermediate occurs during the transition is highly sensitive to the stability of the intermediate against the native and unfolded states. If a protein possesses a higher stabilizing energy in the native state, intermediate species detected kinetically are practically nondetectable by equilibrium methods. That is to say, although the I state is more stable than the U state at early stage of unfolding, the N state is much more stable than the I state, which precludes the population of the I state at equilibrium. During the transition from N to U, the U state becomes more stable than the I state, so that there is eventually no contribution of the I state in the equilibrium unfolding transition. However, if the stabilizing energy in the N state decreases, the N state could not completely preclude the population of the I state at equilibrium. Thus, the apparent difference in the equilibrium unfolding of hen lysozyme between two-state and three-state transitions is probably due to the difference in the relative stability between the N state and the I state. In fact, as can be seen in Figure 3, the accumulation of the I state, which was monitored by near- and far-UV CD, appears to become smaller as ΔG^0_{NU} values increase, indicating that the transition curves approach that of the two-state mechanism.

As cold-induced unfolding, which is well-known phenomenon for globular proteins (*38*), usually occurs below the freezing point of water, detailed studies of the cold-induced unfolded states of proteins have been difficult. As a result, the addition of a denaturant has been often used in order to shift the transition and depress the freezing point of solution (*39*−*41*). Cold-induced unfolding occurs primarily because of the decreased entropic cost of solvating hydrophobic side chains at low temperature (*38*), and the increased hydration of nonpolar residues is expected at lower temperatures, which not only affects the stabilization of I state but in turn also perturbs unfolding behavior. This may be a principal reason the plot of ΔG_{IU} versus temperature appears to increase with the decrease in temperature (Figure 6A).

A number of globular proteins, including α-lactalbumin, are known to show the equilibrium unfolding transition that does not obey the two-state transition model but exhibits a compact intermediate (molten globule state) that has an appreciable amount of secondary structure (*8*, *42*). Structural characterizations of the equilibrium and kinetic intermediates of several proteins have been carried out extensively, and

the results are consistent with a view that the molten globule state is a major intermediate of protein folding (*5*, *8*, *15*, *43*−*45*). According to Kuwajima (*46*), the GdnCl-induced unfolding of the molten globule state of α-lactalbumin shows a cooperative transition, that is, 63% of the unfolding enthalpy change occurs in the transition from the N to the I states and the remaining 37% between the I and U states at 298.2 K. In this study, using the three-state model for GdnCl-induced unfolding of hen lysozyme, 90% of the unfolding enthalpy change occurs in the transition between the N and I states at the same temperature.

Kharakoz and Bychkova (*47*) studied the molten globule of human α-lactalbumin by means of densimetric and ultrasonic techniques. They demonstrated that the hydrophobic core in the molten globule state is highly hydrated and much looser than the core of the native molecule. The small-angle X-ray scattering study has suggested that the compactness of the urea-induced intermediate of hen lysozyme lies halfway between the N and the U conformations, suggesting a significant decrease in tertiary contacts (*26*). Hydrogen-exchange studies on hen lysozyme have revealed that the intermediate formed at the earlier stage of folding reaction shows nativelike secondary structure in the α-domain, whereas the β-domain is largely unstructured (*22*). Recently, Segel et al. (*48*) showed that the kinetic intermediate with helical structure in the α-domain is nearly identical in size and shape with native lysozyme, and the intermediate is much less stable than native state. They suggested that the interconversion between the intermediate and native states requires major structure change in the hydrophobic core of the protein resulting in the substantial change in the environment of some tryptophan residues. As can be seen in Figure 6B, the highest energy barrier for the GdnCl-induced unfolding of hen lysozyme is located between the N and the I states. During the transition with the highest energy barrier between the N and the I states, the exposure of hydrophobic residues to solvent would occur. This process would be largely responsible for acquiring the formation of a hydrophobic core exposed to solvent and for the absence of rigid side-chain packing, hence the cooperativity of protein unfolding. On the other hand, the small ΔH_{IU} and ΔS_{IU} values suggest that hen lysozyme in the I state does not contain substantial region with the tight-packed native structure. This result is consistent with the characteristics on kinetic intermediate found in the refolding pathway of hen lysozyme (*48*).

The lysozyme and α-lactalbumin family can be divided into three subfamilies: non-Ca^{2+}-binding lysozyme (conventional lysozyme), Ca^{2+}-binding lysozyme, and α-lactalbumin (*49*). Certain Ca^{2+}-binding lysozyme (e.g., equine and canine) as well as α-lactalbumin exhibits a stable intermediate state at equilibrium, while non-Ca^{2+}-binding lysozyme is generally known to show a two-state unfolding without accumulation of the I state at equilibrium (*50*). In this study, we have shown that the GdnCl-induced unfolding of hen lysozyme (non-Ca^{2+}-binding lysozyme) at pH 0.9 is well represented by the three-state mechanism in which only N, I, and U states are populated. This result suggests that there is no fundamental distinction in protein unfolding among the lysozyme and α-lactalbumin family. As the thermodynamics and structural aspects of the intermediate states observed in some globular proteins have some relationship with the hierarchical nature of the protein structure (*51*), our results support a hierarchical folding model in which the protein folding/unfolding process proceeds stage by stage, reflecting the hierarchical three-dimensional structure of the folded state (*50*).

REFERENCES

1. Dill, K. A., and Shortle, D. (1991) *Annu. Rev. Biochem. 60*, 795−825.
2. Kim, P. S., and Baldwin, R. L. (1990) *Annu. Rev. Biochem. 59*, 631−660.
3. Creighton, T. E., Darby, N. J., and Kemmink, J. (1996) *FASEB J. 10*, 110−118.
4. Ohgushi, M., and Wada, A. (1983) *FEBS Lett. 164*, 21−24.
5. Kuwajima, K. (1989) *Proteins*: *Struct., Funct., Genet. 6*, 87−103.
6. Dobson, C. M. (1992) *Curr. Opin. Struct. Biol. 2*, 6−12.
7. Haynie, D. T., and Freire, E. (1993) *Proteins*: *Struct., Funct., Genet. 16*, 115−140.
8. Ptitsyn, O. B. (1995) *Adv. Protein Chem. 47*, 83−229
9. Creighton, T. E. (1994) *Nat. Struct. Biol. 1*, 135−138.
10. Roder, H. (1995) *Nat. Struct. Biol. 2*, 817−820.
11. Baldwin, R. L. (1996) *Folding Des. 1*, R1−R8.
12. Dill, S. K., and Chan, H. S. (1997) *Nat. Struct. Biol. 4*, 10−19.
13. Dobson, C. M., Sali, A., and Karplus, M. (1998) *Angew. Chem. 37*, 868−893.
14. Tanford, C. (1970) *Adv. Protein Chem. 24*, 1−95.
15. Dobson, C. M., Evans, P. A., and Radford, S. E. (1994) *Trends Biochem. Sci. 19*, 31−37.
16. Tanford, C. (1968) *Adv. Protein Chem. 23*, 121−282.
17. Aune, K. C., and Tanford, C. (1969) *Biochemistry 8*, 4586−4590.
18. Kuwajima, K. (1996) *FASEB J. 10*, 102−109.
19. Kuwajima, K., Hiraoka, Y., Ikeguchi, M., and Sugai, S. (1985) *Biochemistry 24*, 874−881.
20. Ikeguchi, M., Kuwajima, K., Mitani, M., and Sugai, S. (1986) *Biochemistry 25*, 6965−6972.
21. Miranker, A., Radford, S. E., Karplus, M., and Dobson, C. M. (1991) *Nature 349*, 633−636.
22. Radford, S. E., Dobson, C. M., and Evans, P. A. (1992) *Nature 358*, 302−307.
23. Van Dael, H., Haezebrouck, P., Morozova, L., Arico-Muendel, C., and Dobson, C. M. (1993) *Biochemistry 32*, 11886−11894.
24. Haezebrouck, P., Joniau, M., Van Dael, H., Hooke, S. D, Woodruff, N. D., and Dobson, C. M. (1995) *J. Mol. Biol. 246*, 382−387.
25. Mizuguchi, M., Arai, M., Ke Y., Nitta, K., and Kuwajima, K. (1998) *J. Mol. Biol. 283*, 265−277.
26. Chen, L., Hodgson, K. O., and Doniach, S. (1996) *J. Mol. Biol. 261*, 658−671.
27. Nozaki, Y. (1972) *Methods Enzymol. 26*, 43−50.
28. Fink, A. L., Calciano, L. J., Goto, Y., Kurotsu, T., and Palleros, D. R. (1994) *Biochemistry 33*, 12504−12511.
29. Goto, Y., Takahashi, N., and Fink, A. L. (1990) *Biochemistry 29*, 3480−3488.
30. Pace, C. N. (1986) *Methods Enzymol. 131*, 266−280.
31. Santro, M. M., and Bolen, D. W. (1988) *Biochemistry 27*, 8063−8068.
32. Privalov, P. L. (1979) *Adv. Protein Chem. 33*, 167−241.
33. Pfeil, W., and Privalov, P. L. (1976) *Biophys. Chem. 4*, 41−50.
34. Cooper, A., Eyles, S. J., Radford, S. E., and Dobson, C. M. (1992) *J. Mol. Biol. 225*, 939−943.
35. Privalov, P. L., and Khechinashvili, N. N. (1974) *J. Mol. Biol. 86*, 665−684.
36. Griko, Y. V., Freire, E., Privalov, G., Van Dael, H., and Privalov, P. L. (1995) *J. Mol. Biol. 252*, 447−459.
37. Robson, B., and Pain, R. H. (1976) *Biochem. J. 155*, 331−344.
38. Franks, F. (1995) *Adv. Protein Chem. 46*, 105−139.
39. Chen, B., and Schellman J. A. (1989) *Biochemistry 28*, 685−691.

40. Agashe, V. R., and Udgaonkar, J. B. (1995) *Biochemistry 34*, 3286−3299.
41. Griko, Y. V., Venyaminov, S. Y., and Privalov, P. L. (1989) *FEBS Lett. 244*, 276−278.
42. Privalov, P. L. (1996) *J. Mol. Biol. 258*, 707−725.
43. Hughson, F. M., Wright, P. E., and Baldwin, R. L. (1990) *Science 249*, 1544−1548.
44. Baldwin, R. L. (1993) *Curr. Opin. Struct. Biol. 3*, 84−91.
45. Jennings, P. A., and Wright, P. E. (1993) *Science 262*, 892−896.
46. Kuwajima, K. (1977) *J. Mol. Biol. 114*, 241−258.
47. Kharakoz, D. P., and Bychkova, V. E. (1997) *Biochemistry 36*, 1882−1890.
48. Segel, D. J., Bachmann, A., Hofrichter, J., Hodgson, K. O., Doniach, S., and Kiefhaber, T. (1999) *J. Mol. Biol. 288*, 489−499.
49. Nitta, K., and Sugai, S. (1989) *Eur. J. Biochem. 182*, 111−118.
50. Kuwajima, K., Arai, M., Mizuguchi, M., Koshiba, T., and Nitta, K. (1999) in *Old and New Views of Protein Folding* (Kuwajima, K., and Arai, M., Eds.) pp 135−144, Elsevier Science B. V.
51. Murphy, K. P., Freire, E. (1992) *Adv. Protein Chem. 43*, 313−361.

BI992560K